

Synthesis, Crystal and Electronic Structures, Linear and Nonlinear Optical Properties of Oxyhalides CeHaVIO₄(Ha=Cl, Br; VI=Mo, W)

Zixian Jiao ^a, Jasmine Quah ^a, Tajamul Hussain Syed ^b, Wei Wei ^b, Bingbing Zhang ^c, Fei Wang ^{d,*}, Jian Wang ^{a,*}

^a Department of Chemistry and Biochemistry, Wichita State University, Wichita, Kansas 67260, United States

^b College of Chemistry and Environmental Science, Hebei University, Key Laboratory of Analytical Science and Technology of Hebei Province, Baoding 071002, China

^c Department of Chemistry, Missouri State University, Springfield, Missouri, 65897, United States

Corresponding authors: Fei Wang FeiWang@MissouriState.edu, Jian Wang jian.wang@wichita.edu

1. **Table S1.** Atomic coordinate parameters for CeClMoO₄, CeClWO₄, CeBrMoO₄, and CeBrWO₄.
2. **Table S2.** Selected interatomic distances for CeClWO₄, CeClWO₄, CeBrMoO₄, and CeBrWO₄.
3. **Table S3.** A summary of crystal structure and physical properties of reported compounds within the REHaVIO₄ (Ha=Cl, Br; RE= La-Lu; VI=Mo, W) system.
4. **Table S4.** Comparison of photocurrent density between CeHaVIO₄ (Ha=Cl, Br, VI=Mo, W) compounds and selected reported compounds.
5. **Figure S1.** The optical microscope images of crystals of CeHaVIO₄ (Ha=Cl, Br; VI=Mo, W), from left to right: CeClMoO₄, CeClWO₄, CeBrMoO₄, CeBrWO₄.
6. **Figure S2.** Experimental powder X-ray diffraction results of CeClMoO₄ with theoretical patterns shown at the bottom.
7. **Figure S3.** Experimental powder X-ray diffraction results of CeBrMoO₄ with theoretical patterns shown at the bottom.
8. **Figure S4.** Experimental powder X-ray diffraction results of CeClWO₄ with theoretical patterns shown at the bottom.
9. **Figure S5.** Experimental powder X-ray diffraction results of CeBrWO₄ with theoretical patterns shown at the bottom.
10. **Figure S6.** The (*h*1*l*) planes of the reciprocal lattices of CeClMoO₄ and CeClWO₄.
11. **Figure S7.** Experimental powder X-ray diffraction results of (La_{0.5}Ce_{0.5})ClMoO₄ with theoretical patterns shown at the bottom.
12. **Figure S8.** Experimental powder X-ray diffraction results of (La_{0.5}Ce_{0.5})ClWO₄ with theoretical patterns shown at the bottom.
13. **Figure S9.** Experimental powder X-ray diffraction results of (La_{0.5}Ce_{0.5})BrMoO₄ with theoretical patterns shown at the bottom.

- 14. Figure S10.** Experimental powder X-ray diffraction results of $(La_{0.5}Ce_{0.5})BrWO_4$ with theoretical patterns shown at the bottom.
- 15. Figure S11.** The comparison of bandgaps between $CeHaVIO_4$ ($Ha=Cl, Br; VI=Mo, W$), $LaHaVIO_4$ ($Ha=Cl, Br; VI=Mo, W$), and $(La_{0.5}Ce_{0.5})HaVIO_4$ ($Ha=Cl, Br; VI=Mo, W$).
- 16. Figure S12.** IR spectrum of $CeClMoO_4$ and $CeBrMoO_4$.
- 17. Figure S13.** IR spectrum of $CeClMoO_4$ and $CeBrMoO_4$.
- 18. Figure S14.** DOS and electronic band structure of $LaBrWO_4$ from antiferromagnetic calculation.
- 19. Figure S15.** DOS and electronic band structure of $CeClMoO_4$ from antiferromagnetic calculation.
- 20. Figure S16.** DOS and electronic band structure of $CeClWO_4$ from antiferromagnetic calculation.
- 21. Figure S17.** DOS and electronic band structure of $CeBrMoO_4$ from antiferromagnetic calculation.
- 22. Figure S18.** DOS and electronic band structure of $CeBrWO_4$ from antiferromagnetic calculation.
- 23. Figure S19.** Photocurrent density of three samples of $CeBrMoO_4$.
- 24. Figure S20.** Photocurrent density of three samples of $CeBrWO_4$.
- 25. Figure S21.** Photocurrent density of three samples of $CeClMoO_4$.
- 26. Figure S22.** Photocurrent density of three samples of $CeClWO_4$.
- 27. Figure S23.** The allowed direct transitions of $CeClMoO_4$ sample.
- 28. Figure S24.** The allowed direct transitions of $CeClWO_4$ sample.
- 29. Figure S25.** The allowed direct transitions of $CeBrMoO_4$ sample.
- 30. Figure S26.** The allowed direct transitions of two $CeBrWO_4$ sample.

Table S1. Atomic coordinate parameters for CeClMoO₄, CeClWO₄, CeBrMoO₄, and CeBrWO₄.

Atom	Wyckoff	x	y	z	Occupancy	U_{eq} (Å ²)
CeClMoO ₄						
Ce1	2a	0.49975(3)	0.45044(5)	0.76321(2)	1	0.00708(8)
Ce2	2a	0.91378(3)	0.04967(5)	1.01256(2)	1	0.00692(8)
Mo1	2a	0.06463(5)	0.50589(5)	0.72930(5)	1	0.00512(8)
Mo2	2a	0.34954(5)	0.00201(6)	0.97764(5)	1	0.00599(9)
Cl1	2a	0.68372(17)	1.0092(6)	0.76515(17)	1	0.0135(3)
Cl2	2a	0.73163(19)	0.4896(6)	1.01397(16)	1	0.0125(3)
O1	2a	0.4387(4)	0.2634(5)	1.0444(5)	1	0.0123(7)
O2	2a	0.4444(4)	0.7286(5)	0.9888(6)	1	0.0118(7)
O3	2a	-0.0265(4)	0.7610(4)	0.7927(5)	1	0.0081(6)
O4	2a	-0.0213(4)	0.2304(4)	0.7380(5)	1	0.0069(6)
O5	2a	0.1692(4)	-0.0269(6)	1.0117(4)	1	0.0095(6)
O6	2a	0.2427(4)	0.4984(8)	0.7722(4)	1	0.0100(6)
O7	2a	0.3673(5)	0.0702(6)	0.7612(4)	1	0.0135(9)
O8	2a	0.0570(5)	0.5609(5)	0.5111(3)	1	0.0074(7)
CeClWO ₄						
Ce1	2a	0.74728(5)	0.94769(18)	0.16606(15)	1	0.0073(3)
Ce2	2a	0.24731(5)	0.94579(18)	0.42028(16)	1	0.0073(3)
Ce3	2a	0.96537(3)	0.9986(2)	0.25194(9)	1	0.00419(16)
Ce4	2a	0.46558(3)	1.0029(3)	0.55740(10)	1	0.00432(15)
W1	2a	0.82105(4)	0.5030(3)	0.42716(10)	1	0.00498(19)
W2	2a	0.32184(3)	0.5016(2)	0.23665(10)	1	0.00578(18)
W3	2a	0.09491(7)	1.0031(2)	0.4741(2)	1	0.0032(4)
W4	2a	0.59479(7)	0.9986(2)	0.1670(2)	1	0.0029(4)
Cl1	2a	0.6328(2)	0.9892(14)	0.3584(8)	1	0.0095(8)
Cl2	2a	0.1323(3)	0.9847(17)	0.1082(8)	1	0.0157(13)
Cl3	2a	1.1554(2)	0.5118(16)	0.3704(7)	1	0.0116(11)
Cl4	2a	0.6556(2)	0.4903(16)	0.6216(8)	1	0.0142(11)
O1	2a	0.0070(6)	0.7289(16)	0.3237(16)	1	0.006(2)
O2	2a	0.5075(5)	0.2760(18)	0.0801(18)	1	0.0049(18)
O3	2a	0.0060(6)	0.2776(15)	0.2709(15)	1	0.009(2)
O4	2a	0.7732(5)	0.7537(17)	0.4605(15)	1	0.009(2)
O5	2a	0.5065(4)	0.7298(17)	0.0163(15)	1	0.0037(16)
O6	2a	0.7742(6)	0.239(2)	0.4038(19)	1	0.013(3)

O7	2a	0.2773(5)	0.7570(18)	0.1468(15)	1	0.008(2)
O8	2a	0.4727(4)	0.9236(13)	0.2873(11)	1	0.0052(16)
O9	2a	0.9768(4)	0.9351(14)	0.0282(10)	1	0.014(5)
O10	2a	0.2732(4)	0.2338(15)	0.2119(14)	1	0.0039(15)
O11	2a	0.8130(5)	0.5435(18)	0.1982(13)	1	0.010(2)
O12	2a	0.3204(5)	0.5639(14)	0.4611(10)	1	0.0040(16)
O13	2a	0.4123(4)	0.506(2)	0.2379(14)	1	0.0078(18)
O14	2a	0.9133(5)	0.487(3)	-0.0029(19)	1	0.011(2)
O15	2a	0.3759(5)	-0.008(3)	0.4931(15)	1	0.0036(17)
O16	2a	0.8758(4)	0.028(2)	0.2370(14)	1	0.010(2)
CeBrMoO_4						
Ce1	2a	-0.49130(2)	0.45566(4)	-0.70036(2)	1	0.00712(6)
Ce2	2a	-0.92350(2)	0.95430(4)	-0.44924(2)	1	0.00731(6)
Mo1	2a	-0.06780(3)	0.49756(5)	-0.73530(4)	1	0.00529(7)
Mo2	2a	-0.34715(3)	0.00631(5)	-0.48516(4)	1	0.00581(7)
Br1	2a	-0.67877(5)	1.0015(2)	-0.69846(5)	1	0.01132(10)
Br2	2a	-0.73596(4)	0.4998(2)	-0.94860(5)	1	0.01129(10)
O1	2a	-0.4326(3)	0.2703(5)	-0.9718(4)	1	0.0088(6)
O2	2a	-0.4364(4)	0.7367(5)	-0.9225(4)	1	0.0091(5)
O3	2a	-0.9798(4)	0.7704(5)	-0.7211(5)	1	0.0097(6)
O4	2a	-0.9833(4)	0.2366(5)	-0.6710(4)	1	0.0109(6)
O5	2a	-0.1726(4)	-0.0018(9)	-0.4374(4)	1	0.0136(5)
O6	2a	-0.2431(3)	0.5214(6)	-0.7014(3)	1	0.0080(5)
O7	2a	-0.3583(5)	0.0633(6)	-0.7009(4)	1	0.0111(8)
O8	2a	-0.0563(5)	0.4396(6)	-0.9504(4)	1	0.0113(7)
CeBrWO_4						
Ce1	2a	0.49162(10)	0.45288(12)	0.69896(4)	1	0.00851(19)
Ce2	2a	0.92431(9)	0.95285(12)	0.44826(4)	1	0.00792(19)
W1	2a	0.06693(5)	0.49777(5)	0.72856(6)	1	0.00643(9)
W2	2a	0.34760(5)	0.00404(5)	0.47822(6)	1	0.00602(9)
Br1	2a	0.67902(17)	0.0016(3)	0.69697(11)	1	0.0104(3)
Br2	2a	0.73592(18)	0.4986(3)	0.94727(12)	1	0.0126(3)
O1	2a	0.4375(7)	0.2668(8)	0.9696(9)	1	0.0087(12)
O2	2a	0.4401(7)	0.7376(9)	0.9200(9)	1	0.0097(12)
O3	2a	0.9860(8)	0.7693(8)	0.2793(12)	1	0.0075(11)
O4	2a	0.9871(8)	0.2357(8)	0.6669(8)	1	0.0075(11)
O5	2a	0.1734(8)	0.9996(14)	0.4351(8)	1	0.0065(11)
O6	2a	0.2442(8)	0.5159(16)	0.7042(9)	1	0.0120(15)
O7	2a	0.3609(11)	0.0532(13)	0.7011(6)	1	0.0093(18)

O8	2a	0.0557(12)	0.4339(12)	0.9515(7)	1	0.013(2)
----	----	------------	------------	-----------	---	----------

Table S2. Selected interatomic distances for CeClWO₄, CeClWO₄, CeBrMoO₄, and CeBrWO₄.

Table S2. Selected interatomic distances for CeClWO₄, CeClWO₄, CeBrMoO₄, and CeBrWO₄.

Atom Pairs	Distances (Å)		Atom Pairs	Distances (Å)	
CeClMoO ₄					
Mo1	O3	1.787(3)	Ce2	Cl1	2.9579(15)
	O4	1.796(3)		Cl1	2.9965(16)
	O6	1.735(4)		Cl2	3.086(3)
	O8	1.765(3)		O3	2.485(3)
	O8	2.274(3)		O3	2.547(4)
Mo2	O1	1.817(3)		O4	2.499(4)
	O2	1.827(3)		O4	2.496(3)
	O5	1.752(4)		O5	2.479(4)
	O7	1.774(3)		O8	2.638(4)
	O7	2.299(3)			
Ce1	Cl1	3.102(3)			
	Cl2	2.9880(16)			
	Cl2	2.9923(16)			
	O1	2.552(4)			
	O2	2.472(4)			
	O2	2.469(4)			
	O6	2.472(4)			
	O7	2.540(4)			
CeClWO ₄					
W1	O4	1.797(10)	Ce2	O7	2.576 (12)
	O6	1.798(12)		O7	2.479 (11)
	O11	1.778(11)		O10	2.472 (10)
	O11	2.169(11)		O10	2.469 (10)
	O14	1.784(10)		O12	2.654 (8)
W2	O7	1.810 (10)		O15	2.488 (9)

	O12	1.794 (8)		Cl2	2.980(5)
	O12	2.179(8)		Cl2	2.952 (6)
	O13	1.773(9)		Cl3	3.109 (8)
W3	O1	1.823 (10)	Ce3	O1	2.446(13)
	O3	1.820 (9)		O1	2.460(16)
	O9	1.842(8)		O3	2.497(18)
	O9	2.158 (8)		O3	2.499(16)
	O16	1.746 (9)		O9	2.530(3)
W4	O2	1.831 (10)		O14	2.457(10)
	O5	1.826 (10)		Cl2	3.109 (9)
	O8	2.190 (9)		Cl3	2.987 (5)
	O8	1.823 (9)		Cl3	2.964 (5)
	O15	1.730 (9)	Ce4	O2	2.448(12)
Ce1	O4	2.525 (11)		O2	2.483(14)
	O4	2.500(11)		O5	2.525 (11)
	O6	2.505 (13)		O5	2.458(11)
	O6	2.471 (15)		O8	2.536 (8)
	O11	2.696 (10)		O13	2.464(8)
	O16	2.514 (9)		Cl1	3.133(7)
	Cl1	2.948 (6)		Cl4	2.971 (5)
	Cl1	2.965 (5)		Cl4	2.985 (6)
	Cl4	3.126 (8)			

CeBrMoO₄

Mo1	O3	1.810(3)	Ce2	Br1	3.1321(5)
	O4	1.805(3)		Br1	3.1380(5)
	O6	1.741(3)		Br2	3.2172(12)
	O8	1.764(3)		O3	2.493(3)
	O8	2.320(3)		O3	2.496(3)
Mo2	O1	1.818(3)		O4	2.493(3)
	O2	1.804(3)		O4	2.5634(3)
	O5	1.750(4)		O5	2.451(4)
	O7	1.768(3)		O8	2.635(4)
	O7	2.321(3)			

Ce1	Br1	3.2167(12)			
	Br2	3.1245(5)			
	Br2	3.1433(5)			
	O1	2.499(3)			
	O1	2.499(3)			
	O2	2.480(3)			
	O6	2.457(3)			
	O7	2.628(4)			
CeBrWO ₄					
W1	O3	1.797(5)	Ce2	Br1	3.1393(16)
	O4	1.808(5)		Br1	3.1501(16)
	O6	1.765(8)		Br2	3.257(2)
	O8	1.814(5)		O3	2.505(7)
	O8	2.239(5)		O3	2.511(6)
W2	O1	1.835(5)		O4	2.491(6)
	O2	1.842(6)		O4	2.573(6)
	O5	1.755(7)		O5	2.478(8)
	O7	1.798(5)		O8	2.633(9)
	O7	2.230(5)			
Ce1	Br1	3.2514(18)			
	Br2	3.2514(18)			
	Br2	3.1466(17)			
	O1	2.474(7)			
	O2	2.521(6)			
	O2	2.486(6)			
	O2	2.537(7)			
	O6	2.473(8)			
	O7	2.697(9)			

Table S3. A summary of crystal structure and physical properties of reported compounds within the REHaVIO₄ (Ha=Cl, Br; RE= La-Lu; VI=Mo, W) system.

Compounds	Space Group	Unit cell parameters	Structure Type	Physical Properties	Basic building units	Reference

						e
LaClMoO ₄	<i>P2</i> ₁ / <i>c</i>	19.2055(18) ×5.8046(5) ×8.0382(7) $\beta=90.040(6)$ ° monoclinic V=896.10 Å ³	CeClWO ₄		[LaO ₆ Cl ₃] [MoO ₅]	1
CeClMoO ₄	<i>P2</i> ₁ / <i>c</i>	19.1228(18) ×5.7992(5) ×7.9591(7) $\beta=90.037(6)$ ° monoclinic V= 882.64 Å ³	CeClMoO ₄	Paramagnetic, absence of any significant long range order even at 1.8 K.	[CeO ₆ Cl ₃] [MoO ₅]	1
NdClMoO ₄	<i>Pbam</i>	19.9161(9) ×6.9379(3) ×7.4253(3) orthorhombic V= 1026.00 Å ³	NdClMoO ₄		[NdO ₆ Cl ₂] [MoO ₄]	2
YbClMoO ₄	<i>C12/m</i>	10.1019(5) ×7.1334(3) ×6.7756(3) $\beta= 107.408(2)$ ° monoclinic V=465.89 Å ³	YbClMoO ₄		[YbO ₆ Cl ₂] [MoO ₄]	3
LaClWO ₄	<i>Pbc2</i> ₁	5.893(3) ×7.856(4) ×19.270(9) orthorhombic V= 892.11 Å ³	LaClWO ₄	Eg=4.0(2) eV (La _{0.98} Sm _{0.02})ClWO ₄ : ⁴ G _{7/2} -> ⁶ H _{9/2} , ⁴ G _{5/2} -> ⁶ H _{7/2} excited by 404 nm. (La _{0.99} Eu _{0.01})ClWO ₄ : ⁵ D ₀ -> ⁷ F ₁ , ⁵ D ₀ -> ⁷ F ₂ , excited by 394 nm. (La _{0.995} Tb _{0.005})ClWO ₄ : ⁵ D ₄ -> ⁷ F ₆ , ⁵ D ₄ to ⁷ F ₅ excited by 320 nm.	[LaO ₆ Cl ₃] [MoO ₅]	4
LaClWO ₄	<i>Pmcn</i>	5.893(3) ×3.928(2) × 19.270(9) orthorhombic V= 446.06 Å ³	LaClWO ₄		[LaO ₅ Cl ₄] [MoO ₅]	4
LaBrMoO ₄	<i>P1c1</i>	9.8197(4) × 5.8183(2) × 8.1051(3) $\beta=90.039(3)$ ° monoclinic V=463.08 Å ³	LaBrMoO ₄		[LaO ₆ Br ₃] [MoO ₅]	5
CeBrMoO ₄	<i>P1c1</i>	9.7691(4) ×5.8146(2) × 8.0259(3) $\beta=90.004(3)$ ° monoclinic V=455.90 Å ³	LaBrMoO ₄		[CeO ₆ Br ₃] [MoO ₅]	5
CeClMoO ₄	<i>P1c1</i>	9.55130(10)×5.793×7.94950(10) $\beta=90.0140(7)$ ° monoclinic		E _g =2.9 (1) eV	[CeO ₆ Cl ₃] [MoO ₅]	Th is w or

		V=439.851(7) Å ³				k
CeClWO ₄	P1c1	19.6059(2) 5.89450(10) 7.80090(10) $\beta=101.4746(8)$ ° monoclinic V=883.51(2) Å ³		E _g =3.1 (1) eV	[CeO ₆ Cl ₃] [MoO ₅]	Th is w or k
CeBrMoO ₄	P1c1	9.77750(10)× 5.82090(10) × 8.03220(10) $\beta=90.0106$ ° monoclinic V=457.143(11) Å ³		E _g =2.8 (1) eV	[CeO ₆ Br ₃] [MoO ₅]	Th is w or k
CeBrWO ₄	P1c1	9.87830(10)× 5.92230(10) × 7.93940(10) $\beta=90.0083$ ° monoclinic V=464.473(11) Å ³		E _g =3.0 (1) eV	[CeO ₆ Br ₃] [WO ₅]	Th is w or k
LuBrWO ₄	P -1	5.9292(3) ×7.1869(4) ×6.8443(4) $\alpha=93.637(3)$ ° $\beta=102.944(3)$ ° $\gamma=121.875(3)$ ° triclinic V= 235.49Å ³	LuBrWO ₄		[LuO ₆ Br] [LuO ₄ Br ₃] [WO ₄]	6
TmClWO ₄	P -1	5.9638(3) × 7.2110(4) ×6.8551(4) $\alpha=93.243(3)$ ° $\beta=103.066(3)$ ° $\gamma=121.995(3)$ ° triclinic V= 237.93Å ³	LuClMoO ₄		[TmO ₅ Cl ₂] [WO ₄]	7
YbClWO ₄	P -1	5.9235(3) ×7.1845(4) ×6.8448(4) $\alpha=93.523(3)$ ° $\beta=103.001(3)$ ° $\gamma=121.745(3)$ ° triclinic V= 235.61Å ³	LuClMoO ₄	E _g =4.23 eV	[YbO ₅ Cl ₂] [WO ₄]	7
LuClWO ₄	P -1	5.9292(3) × 7.1869(4) × 6.8443(4) $\alpha=93.637(3)$ ° $\beta=102.944(3)$ °	LuClMoO ₄	LuClWO ₄ :Eu ³⁺ : ⁵ D ₀ -> ⁷ F ₂ to ⁷ F ₁	[LuO ₅ Cl ₂] [WO ₄]	7

		° γ=121.875(3) ° triclinic V= 235.48 Å³				
LuClMoO ₄	P -1	5.9142(2) ×7.1619(3) × 6.8144(3) α=93.724(2) ° β=102.463(2) ° γ=122.134(2) ° triclinic V=232.95 Å³	LuClMoO ₄		[LuO ₅ Cl ₂] [MoO ₄]	3
SmClMoO ₄	C12/m1	10.3480(5) ×7.3602(3) × 6.9084(3) β=106.677(2) ° monoclinic V= 504.04 Å³	GdClWO ₄		[SmO ₆ Cl ₂] [MoO ₄]	3
EuClMoO ₄	C12/m1	10.3161(5) × 7.3280(3) × 6.8878(3) β=106.773(2) ° monoclinic V= 498.54 Å³	GdClWO ₄	⁵ D ₀ -> ⁷ F ₀ to ⁷ F ₄ emissions of Eu ³⁺ in the visible region	[EuO ₆ Cl ₂] [MoO ₄]	3
GdClMoO ₄	C12/m1	10.2890(5) ×7.3051(3) ×6.8711(3) β= 106.864(2) ° monoclinic V= 494.24 Å³	GdClWO ₄	GdCl[MoO ₄] is a close-to-ideal paramagnet with no hint to magnetic interactions down to 1.8 K.	[GdO ₆ Cl ₂] [MoO ₄]	3
TbClMoO ₄	C12/m1	10.2517(5) ×7.2682(3) × 6.8497(3) β=106.963(2) ° monoclinic V= 488.18 Å³	GdClWO ₄	⁵ D ₄ -> ⁷ F ₀ to ⁷ F ₆ transitions of Tb ³⁺ in the visible region	[TbO ₆ Cl ₂] [MoO ₄]	3
DyClMoO ₄	C12/m1	10.2199(5) ×7.2367(3) × 6.8322(3) β=107.057(2) ° monoclinic V= 483.07 Å³	GdClWO ₄	Paramagnet, absence of any long range order down to 1.8 K.	[DyO ₆ Cl ₂] [MoO ₄]	3
HoClMoO ₄	C12/m1	10.1900(5) ×7.2147(3) ×6.8148(3) β=107.142(2) ° V= 478.75 Å³	GdClWO ₄		[HoO ₆ Cl ₂] [MoO ₄]	3
ErClMoO ₄	C12/m1	10.1536(5) ×7.1874(3)	GdClWO ₄		[ErO ₆ Cl ₂] [MoO ₄]	3

		$\times 6.7964(3)$ $\beta=107.236(2)$ ° monoclinic $V= 473.71 \text{ \AA}^3$				
TmClMoO ₄	C12/m1	$10.1327(5)$ $\times 7.1591(3) \times$ $6.7850(3)$ $\beta=107.320(2)$ ° monoclinic $V= 469.87 \text{ \AA}^3$	GdClWO ₄		[TmO ₆ Cl ₂] [MoO ₄]	3
GdClWO ₄	C12/m1	$10.3219(5) \times 7$.3249(3) × 6.8888(3) $\beta=107.229(2)$ ° monoclinic $V= 497.46 \text{ \AA}^3$	GdClWO ₄	GdClWO ₄ :Eu ³⁺ : ⁵ D ₀ -> ⁷ F ₂ to ⁷ F ₁		2, 7
TbClWO ₄	C12/m1	$10.2806(5) \times$ 7.2858(3) × 6.8713(3) $\beta=107.293(2)$ ° monoclinic $V= 491.41 \text{ \AA}^3$	GdClWO ₄	⁵ D ₄ -> ⁷ F ₅ to ⁷ F ₆ emissions of Tb ³⁺ in the visible region $E_g=4.24 \text{ eV}$		7
DyClWO ₄	C12/m1	$10.2524(5) \times$ 7.2583(3) × 6.8561(3) $\beta= 107.401(2)$ ° monoclinic $V= 486.84 \text{ \AA}^3$	GdClWO ₄			7
HoClWO ₄	C12/m1	$10.2154(5) \times$ 7.2303(3) × 6.8333(3) $\beta= 107.470(2)$ ° monoclinic $V= 481.43 \text{ \AA}^3$	GdClWO ₄			7
ErClWO ₄	C12/m1	$10.1877(5) \times$ 7.2053(3) $\times 6.8201(3)$ $\beta= 107.561(2)$ ° monoclinic $V= 477.30 \text{ \AA}^3$	GdClWO ₄			7
PrBrMoO ₄	P -1	$6.9795(2) \times$ 7.4069(2) $\times 11.2088(4)$ $\alpha=$ 105.945(2) ° $\beta= 106.702(2)$ ° $\gamma= 92.355(2)$ ° triclinic $V=$ $92.355(2) \text{ \AA}^3$	YbBrMoO ₄		[PrO ₄ Br ₃] [PrO ₆ Br] [MoO ₄]	8
NdBrMoO ₄	P -1	6.9529(2)	YbBrMoO ₄		[NdO ₄ Br ₃]	8

		$\times 7.3756(2)$ $\times 11.1770(4)$ $\alpha =$ 106.061(2) ° $\beta = 106.743(2)$ ° $\gamma = 92.329(2)$ ° triclinic $V = 522.92 \text{ \AA}^3$		[NdO ₆ Br] [MoO ₄]	
SmBrMoO ₄	<i>P</i> -1	$6.9138(2)$ $\times 7.3078(2)$ $\times 11.1045(4)$ $\alpha =$ 106.061(2) ° $\beta = 106.983(2)$ ° $\gamma = 92.239(2)$ ° triclinic $V = 511.24 \text{ \AA}^3$	YbBrMoO ₄	[SmO ₄ Br ₃] [SmO ₆ Br] [MoO ₄]	8
GdBrMoO ₄	<i>P</i> -1	$6.8853(2) \times$ 7.2628(2) $\times 11.0593(4)$ $\alpha =$ 106.142(2) ° $\beta = 107.098(2)$ ° $\gamma = 92.260(2)$ ° triclinic $V = 503.31 \text{ \AA}^3$	YbBrMoO ₄	[GdO ₄ Br ₃] [GdO ₆ Br] [MoO ₄]	8
TbBrMoO ₄	<i>P</i> -1	$6.8664(2) \times$ 7.2206(2) $\times 10.9705(4)$ $\alpha =$ 105.574(2) ° $\beta = 107.262(2)$ ° $\gamma = 92.516(2)$ ° triclinic $V = 495.81 \text{ \AA}^3$	YbBrMoO ₄	[TbO ₄ Br ₃] [TbO ₆ Br] [MoO ₄]	8
DyBrMoO ₄	<i>P</i> -1	$6.8565(2) \times$ 7.1913(2) $\times 10.9319(4)$ $\alpha =$ 105.397(2) ° $\beta = 107.332(2)$ ° $\gamma = 92.750(2)$ ° triclinic $V = 491.33 \text{ \AA}^3$	YbBrMoO ₄	[DyO ₄ Br ₃] [DyO ₆ Br] [MoO ₄]	8
HoBrMoO ₄	<i>P</i> -1	$6.8516(2)$ $\times 7.1793(2)$ $\times 10.8832(4)$ $\alpha =$ 105.0310(10) ° $\beta = 107.3420(10)$ ° $\gamma =$	YbBrMoO ₄	[HoO ₄ Br ₃] [HoO ₆ Br] [MoO ₄]	8

		93.1450(10) ° triclinic V= 488.42 Å ³				
ErBrMoO ₄	P -1	6.8481(2) ×7.1600(2) ×10.8135(4) α = 104.4300(10) ° β =107.4550(10) ° γ = 93.6640(10) ° triclinic V= 484.29 Å ³	YbBrMoO ₄		[ErO ₄ Br ₃] [ErO ₆ Br] [MoO ₄]	8
TmBrMoO ₄	P -1	6.8610(2) × 7.1504(2) ×10.7455(4) α = 103.613(2) ° β =107.627(2) ° γ = 94.238(2) ° triclinic V= 482.26 Å ³	YbBrMoO ₄		[TmO ₄ Br ₃] [TmO ₆ Br] [MoO ₄]	8
YbBrMoO ₄	P -1	6.8600(2) × 7.1324(2) ×10.6973(4) α = 103.2340(10) ° β =107.6650(10) ° γ = 94.7120(10) ° triclinic V= 478.95 Å ³	YbBrMoO ₄		[YbO ₄ Br ₃] [YbO ₆ Br] [MoO ₄]	8
LuBrMoO ₄	P -1	6.8594(2) ×7.1270(2) ×10.6618(4) α =102.954(2) ° β =107.688(2) ° γ =95.034(2) ° triclinic V= 477.08 Å ³	YbBrMoO ₄		[LuO ₄ Br ₃] [LuO ₆ Br] [MoO ₄]	8
GdBrWO ₄	P -1	6.9118(4) × 7.2772(4) ×11.0647(6) α =105.518(4) ° β =107.514(4) ° γ =92.650(4) ° triclinic V= 506.50 Å ³	YbBrMoO ₄			9
TbBrWO ₄	P -1	6.9050(4) ×	YbBrMoO ₄			9

		7.2425(4) x10.9718(6) α =104.663(4) ° β =107.754(4) ° γ =93.058(4) ° triclinic V= 500.44 Å³				
DyBrWO ₄	<i>P</i> -1	6.8970(4) x7.2193(4) x10.9266(6) α =104.366(4) ° β =107.811(4) ° γ =93.460(4) ° triclinic V= 496.27 Å³	YbBrMoO ₄			9
ErBrWO ₄	<i>P</i> -1	6.8976(4) x7.1902(4) x10.8208(6) α =103.365(4) ° β =107.994(4) ° γ =94.347(4) ° triclinic V= 490.26 Å³	YbBrMoO ₄			9
HoBrWO ₄	<i>P</i> -1	6.8957(4) x 7.2050(4) x10.8732(6) α =103.885(4) ° β =107.892(4) ° γ =93.915(4) ° triclinic V= 493.13 Å³	YbBrMoO ₄	without any magnetic ordering above 60 K		9
TmBrWO ₄	<i>P</i> -1	6.8927(3) x7.1725(4) x10.7748(6) α =102.922(4) ° β =108.122(4) ° γ =94.577(4) ° triclinic V= 486.98 Å³	YbBrMoO ₄			9
YbBrWO ₄	<i>P</i> -1	6.8857(4) x7.1496(4) x10.7432(6) α =102.715(4) ° β =108.201(4) ° γ =94.859(4) ° triclinic	YbBrMoO ₄			9

		V= 483.33 Å ³			
--	--	--------------------------	--	--	--

Table S4. Comparison of photocurrent density between CeHaVIO₄ (Ha=Cl, Br, VI=Mo, W) compounds and selected reported compounds.

Compounds	Current Density (μA/cm ²)	Reference
Rb ₂ Ba ₃ Cu ₂ Sb ₂ S ₁₀	0.006	10
Pb ₅ Sn ₃ S ₁₀ Cl ₂	0.019	11
RbIn ₄ S ₆ Cl	0.029	11
BaCuSbSe ₃	0.03	12
BaCuSbS ₃	0.055	12
Sr ₆ Cd ₂ Sb ₆ S ₁₀ O ₇	0.065	13
Eu ₃ Gd ₆ MgS ₂ B ₂₀ O ₄₁	0.12	14
CeBrWO ₄	0.1615	This work
LaNi _{0.8} Fe _{0.2} O ₃	0.25	15
CeBrMoO ₄	0.3321	This work
Cs ₂ CuBr ₄	0.5	16
CeClWO ₄	0.5527	This work
CeClMoO ₄	0.747	This work
Eu ₈ In _{17.33} S ₃₄	1	17
Tm ₄ S ₄ Te ₃	1.1	18
Eu _{5.4} Sm _{3.6} MgS ₂ B ₂₀ O ₄₁	1.62	14
Zn ₄ B ₆ O ₁₂ S	2.1	19
Ho ₄ S ₄ Te ₃	2.2	18
Gd ₄ S ₄ Te ₃	2.3	18
Sr ₂ YbRuO ₆	5.5	20
Rb ₂ CuSb ₇ S ₁₂	10	21
Ba ₃ HgGa ₂ S ₇	12.2	22
La _{2.1} Bi _{2.9} Ti ₂ O ₁₁ Cl	15	23
Ba ₂ ZnSe ₃	25	24
BaAu ₂ S ₂	30	25

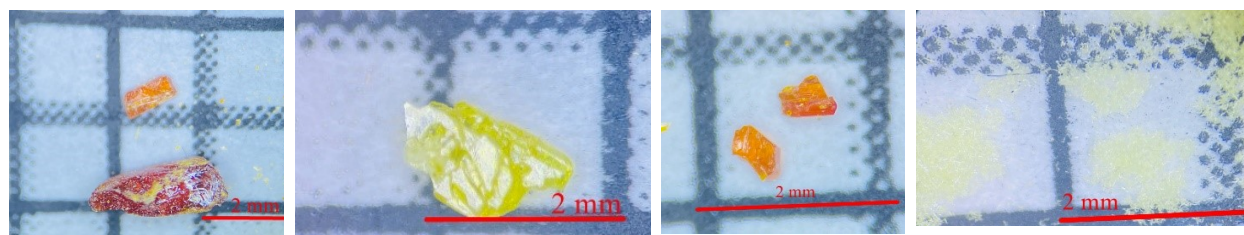


Figure S1. The optical microscope images of crystals of CeHaVIO₄ (Ha=Cl, Br; VI=Mo, W), from left to right: CeClMoO₄, CeClWO₄, CeBrMoO₄, CeBrWO₄.

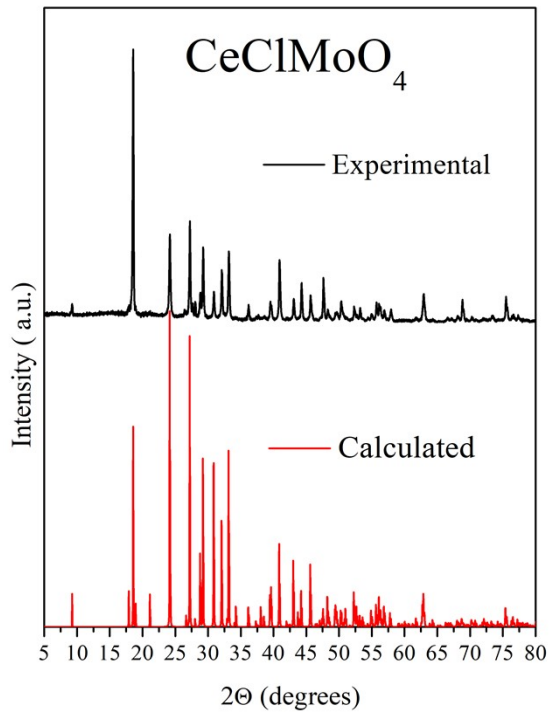


Figure S2. Experimental powder X-ray diffraction results of CeClMoO₄ with theoretical patterns shown at the bottom.

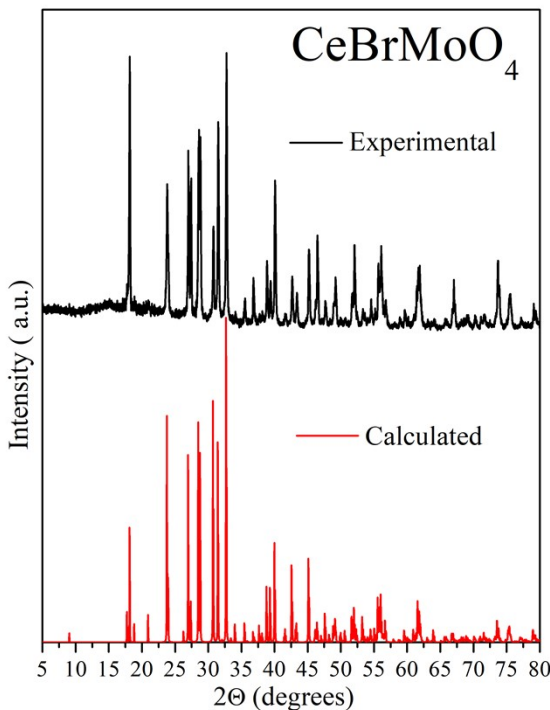


Figure S3. Experimental powder X-ray diffraction results of CeBrMoO₄ with theoretical patterns shown at the bottom.

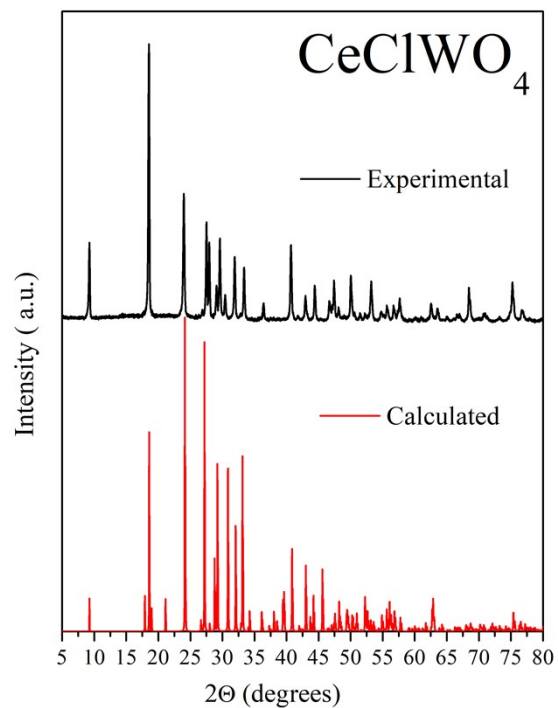


Figure S4. Experimental powder X-ray diffraction results of CeClWO₄ with theoretical patterns shown at the bottom.

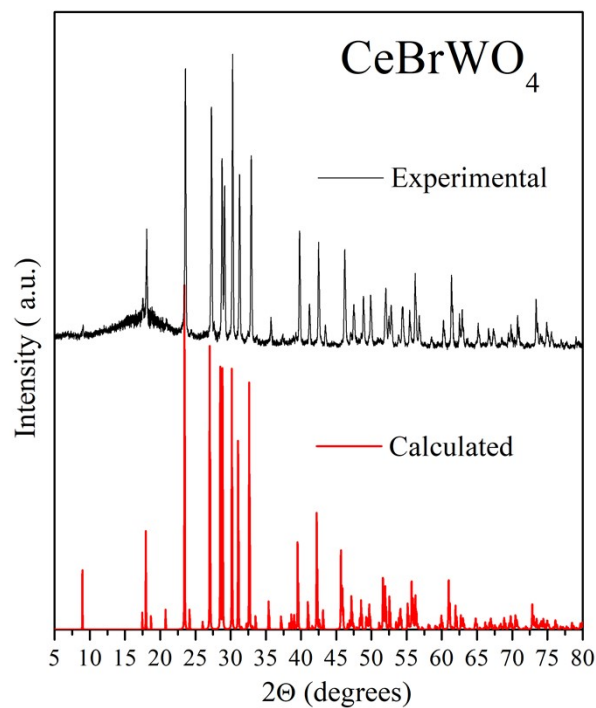


Figure S5. Experimental powder X-ray diffraction results of CeBrWO₄ with theoretical patterns shown at the bottom.

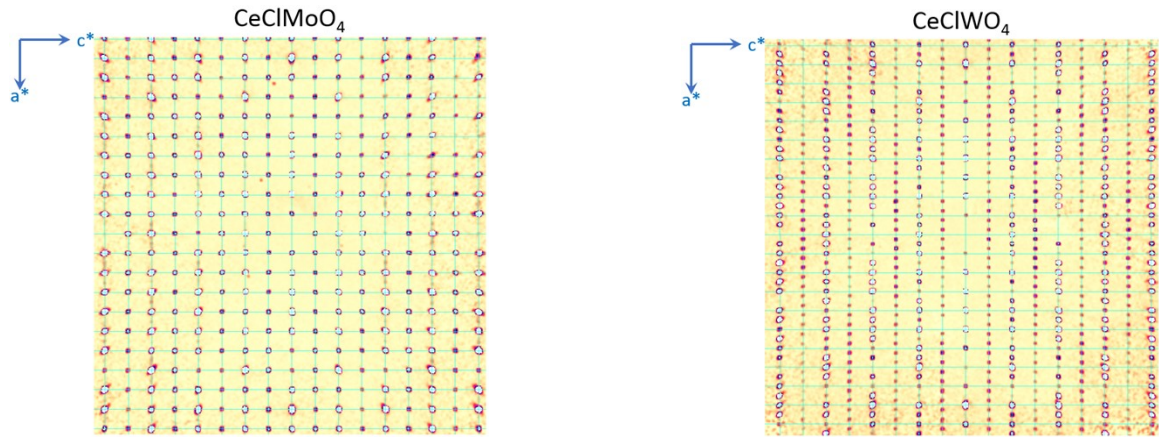


Figure S6. The ($h1l$) planes of the reciprocal lattices of CeClMoO₄ and CeClWO₄.

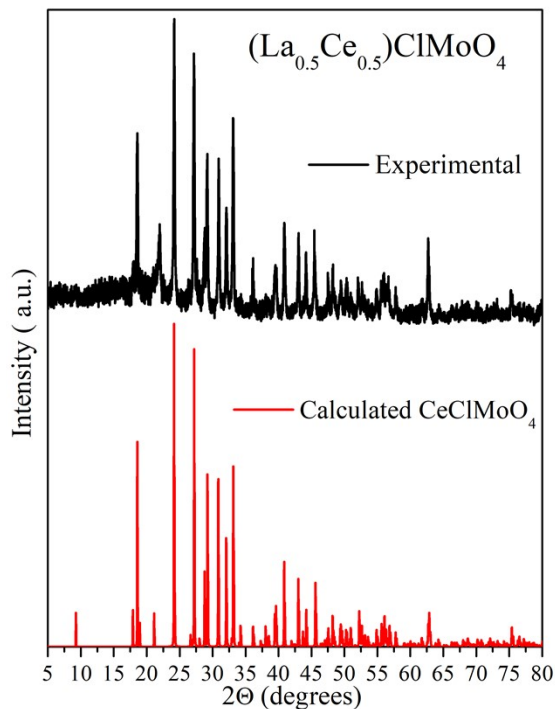


Figure S7. Experimental powder X-ray diffraction results of (La_{0.5}Ce_{0.5})ClMoO₄ with theoretical patterns shown at the bottom.

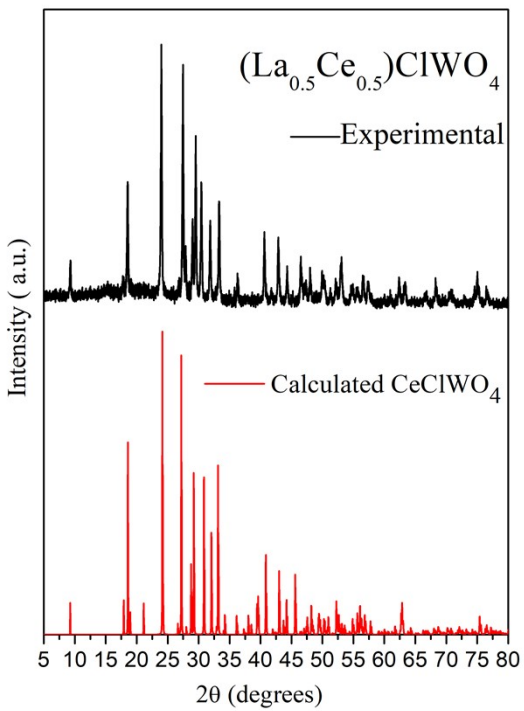


Figure S8. Experimental powder X-ray diffraction results of $(\text{La}_{0.5}\text{Ce}_{0.5})\text{ClWO}_4$ with theoretical patterns shown at the bottom.

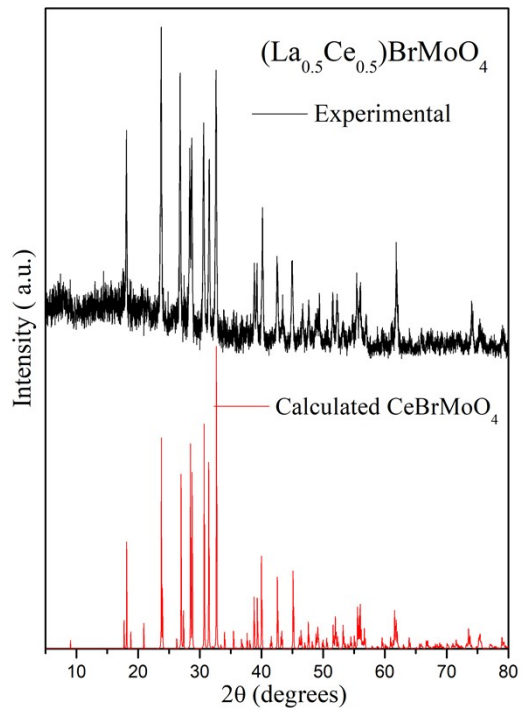


Figure S9. Experimental powder X-ray diffraction results of $(\text{La}_{0.5}\text{Ce}_{0.5})\text{BrMoO}_4$ with theoretical patterns shown at the bottom.

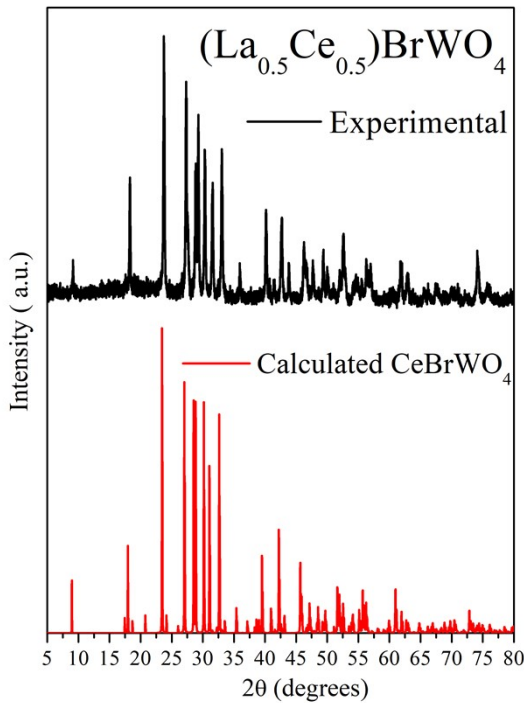


Figure S10. Experimental powder X-ray diffraction results of $(\text{La}_{0.5}\text{Ce}_{0.5})\text{BrWO}_4$ with theoretical patterns shown at the bottom.

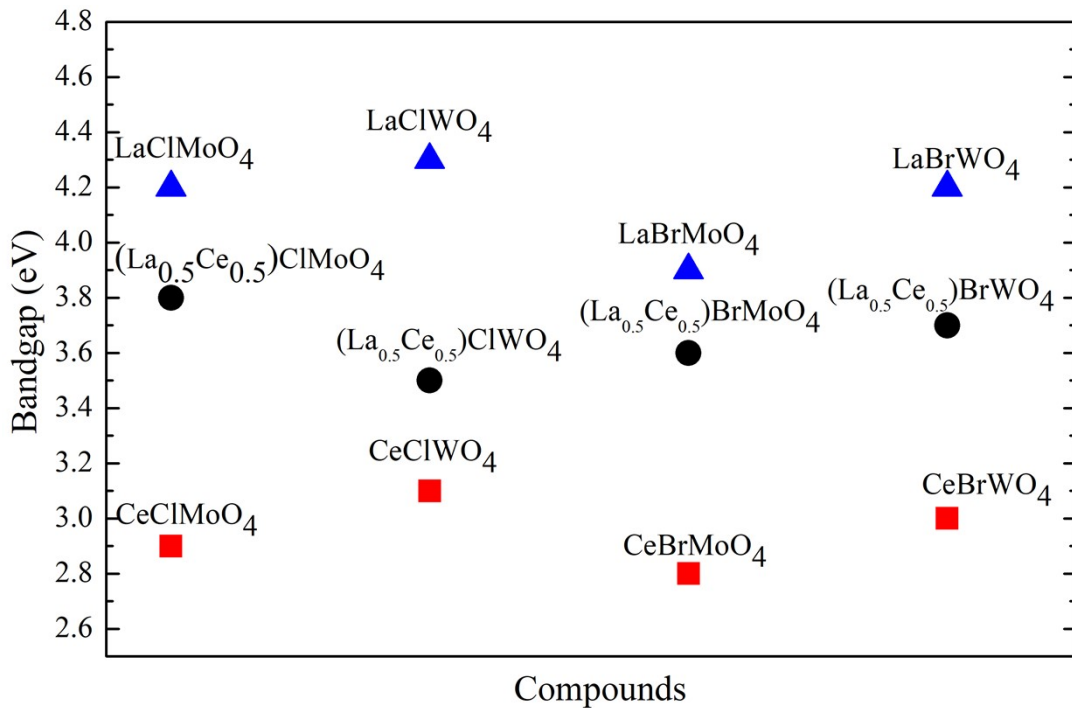


Figure S11. The comparison of bandgaps between CeHaVIO_4 ($\text{Ha}=\text{Cl}, \text{Br}; \text{VI}=\text{Mo}, \text{W}$), LaHaVIO_4 ($\text{Ha}=\text{Cl}, \text{Br}; \text{VI}=\text{Mo}, \text{W}$), and $(\text{La}_{0.5}\text{Ce}_{0.5})\text{HaVIO}_4$ ($\text{Ha}=\text{Cl}, \text{Br}; \text{VI}=\text{Mo}, \text{W}$).

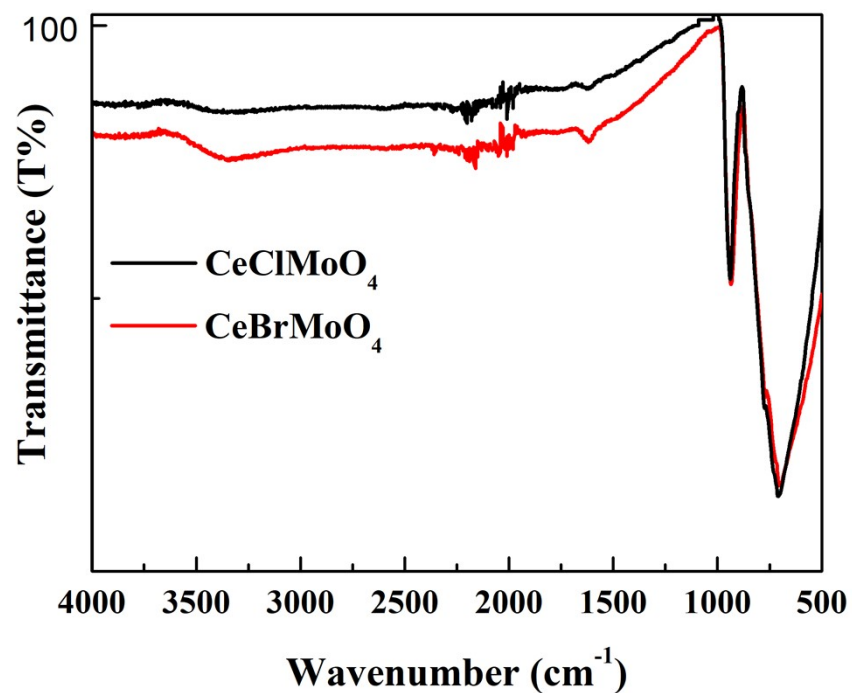


Figure S12. IR spectrum of CeClMoO_4 and CeBrMoO_4 .

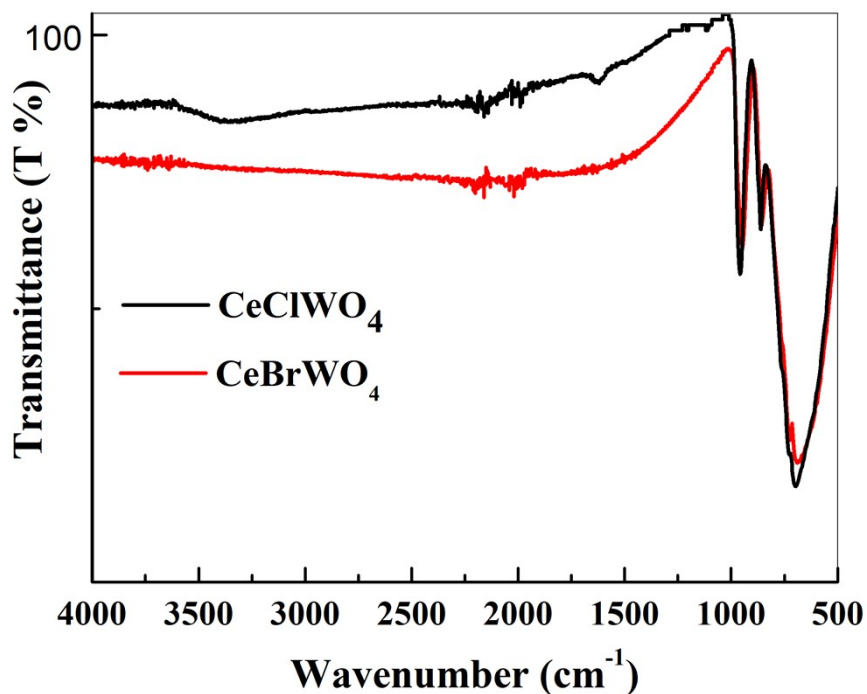


Figure S13. IR spectrum of CeClMoO_4 and CeBrMoO_4 .

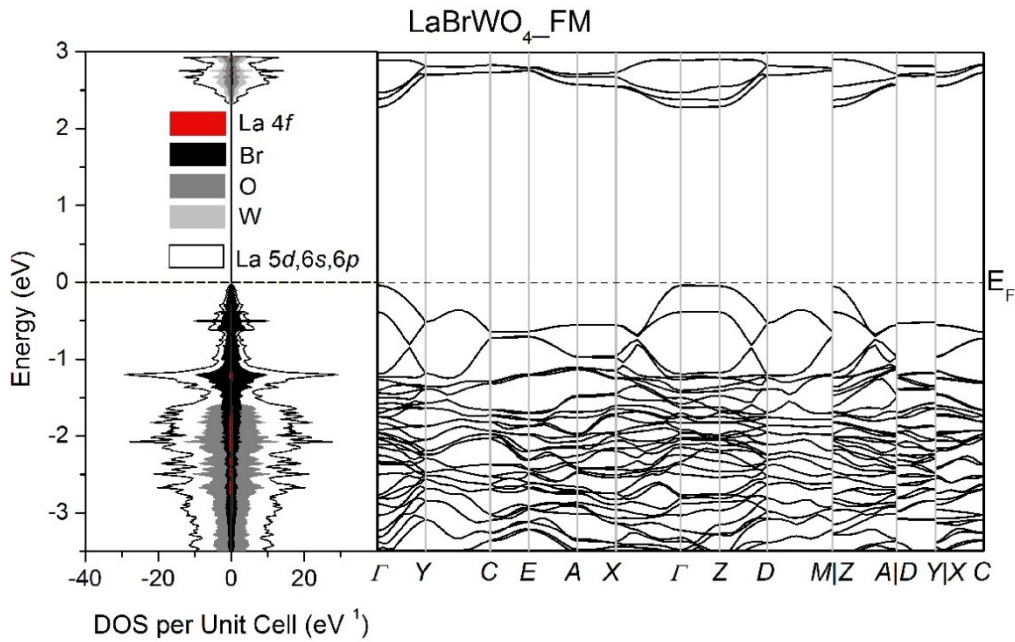


Figure S14. DOS and electronic band structure of LaBrWO_4 from antiferromagnetic calculation.

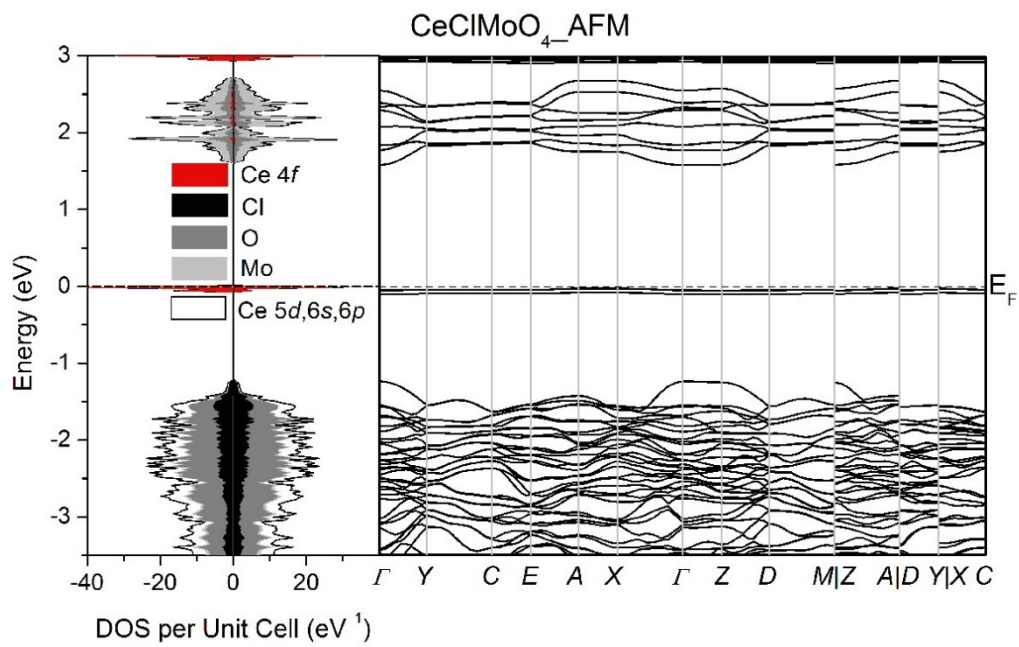


Figure S15. DOS and electronic band structure of CeClMoO_4 from antiferromagnetic calculation.

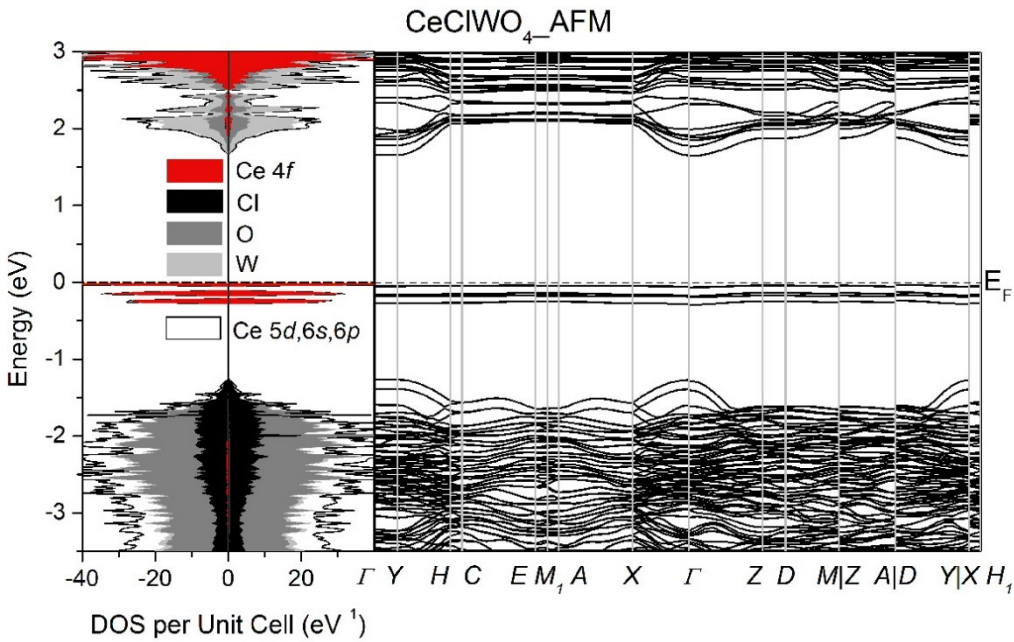


Figure S16. DOS and electronic band structure of CeCl₂WO₄ from antiferromagnetic calculation.

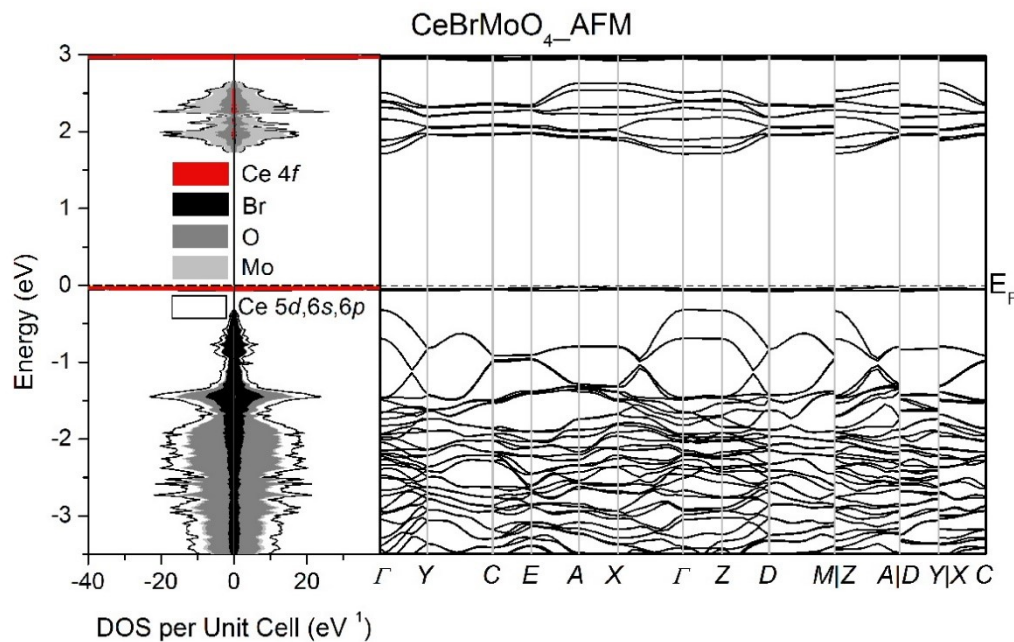


Figure S17. DOS and electronic band structure of CeBrMoO₄ from antiferromagnetic calculation.

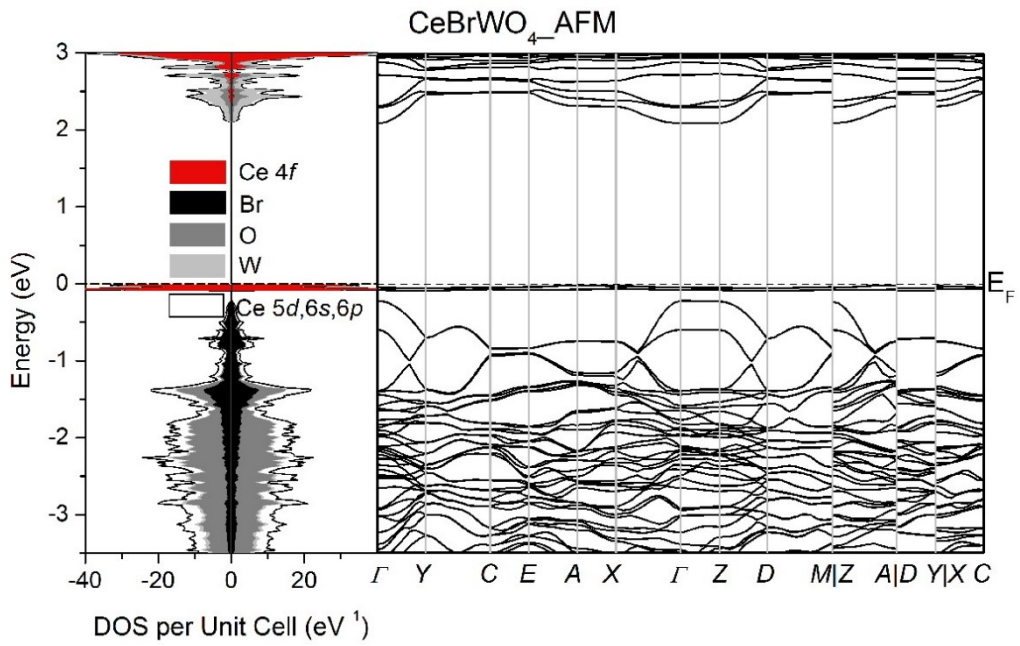


Figure S18. DOS and electronic band structure of CeBrWO_4 from antiferromagnetic calculation.

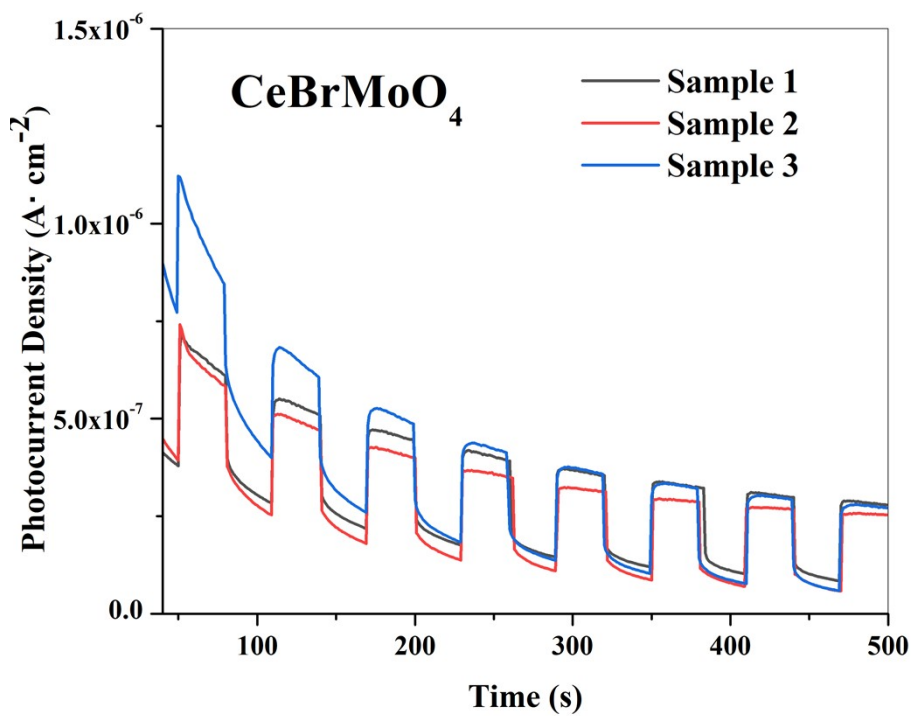


Figure S19. Photocurrent density of three samples of CeBrMoO_4 .

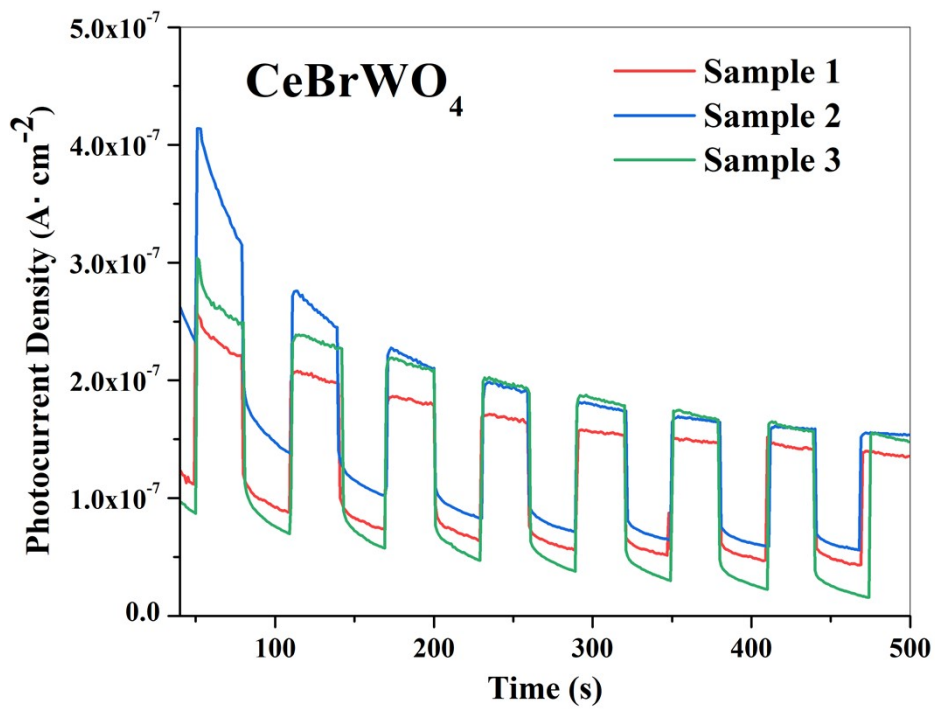


Figure S20. Photocurrent density of three samples of CeBrWO₄.

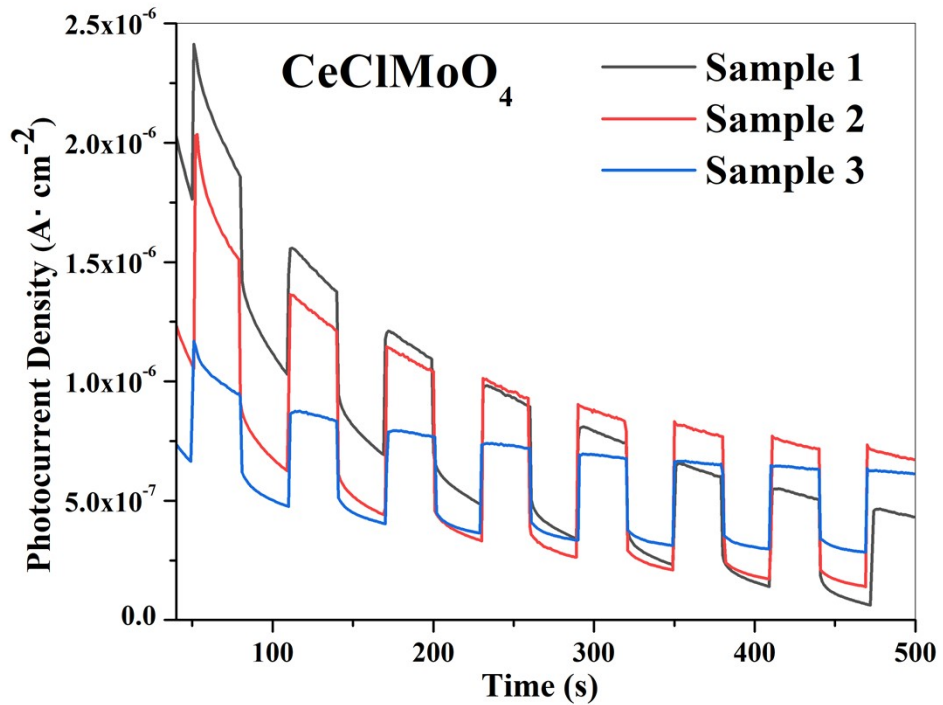


Figure S21. Photocurrent density of three samples of CeClMoO₄.

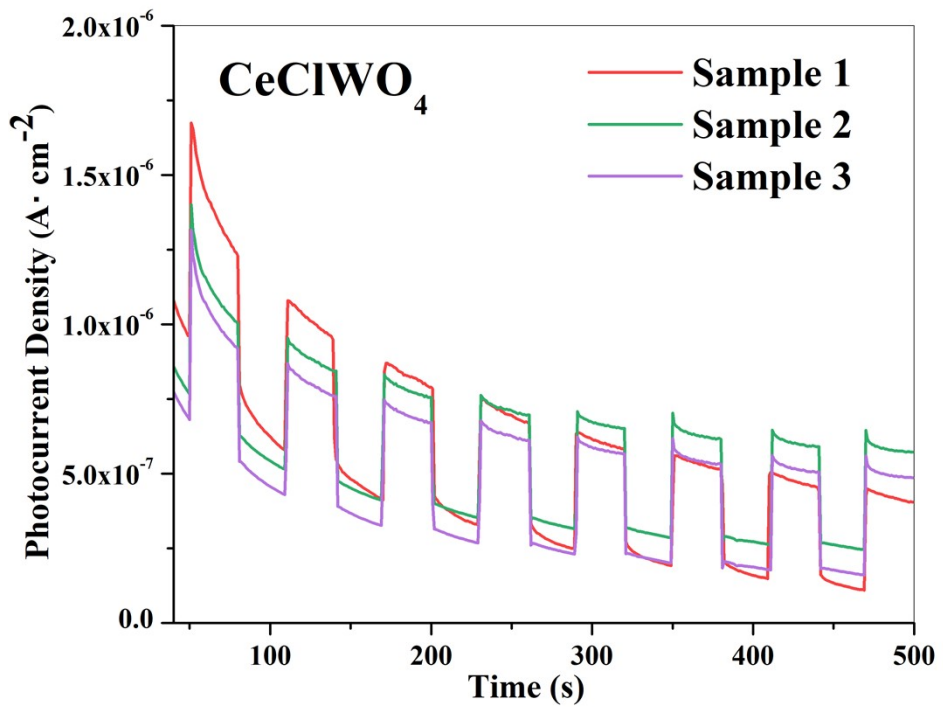


Figure S22. Photocurrent density of three samples of CeClWO₄.

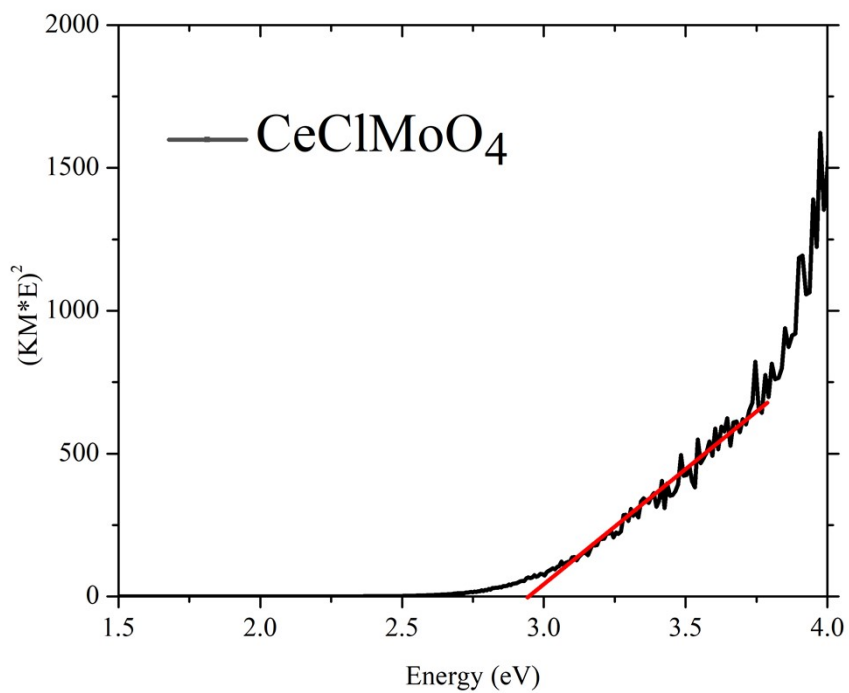


Figure S23. The allowed direct transitions of CeClMoO₄ sample.

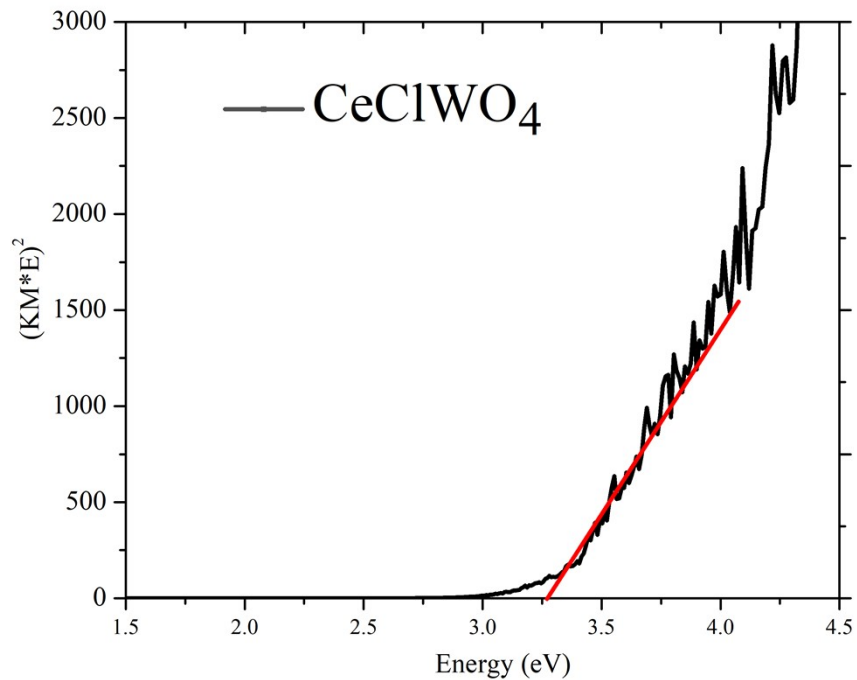


Figure S24. The allowed direct transitions of CeClWO₄ sample.

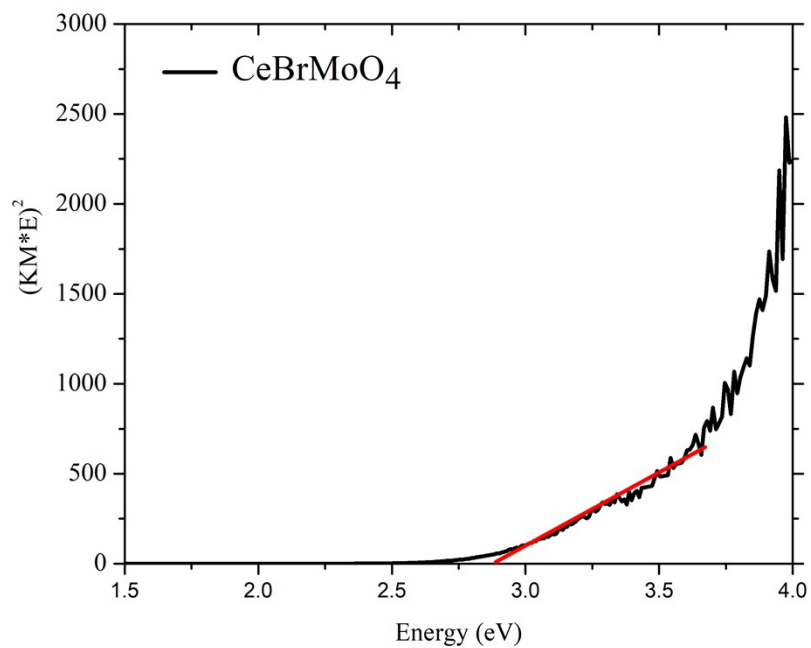


Figure S25. The allowed direct transitions of CeBrMoO₄ sample.

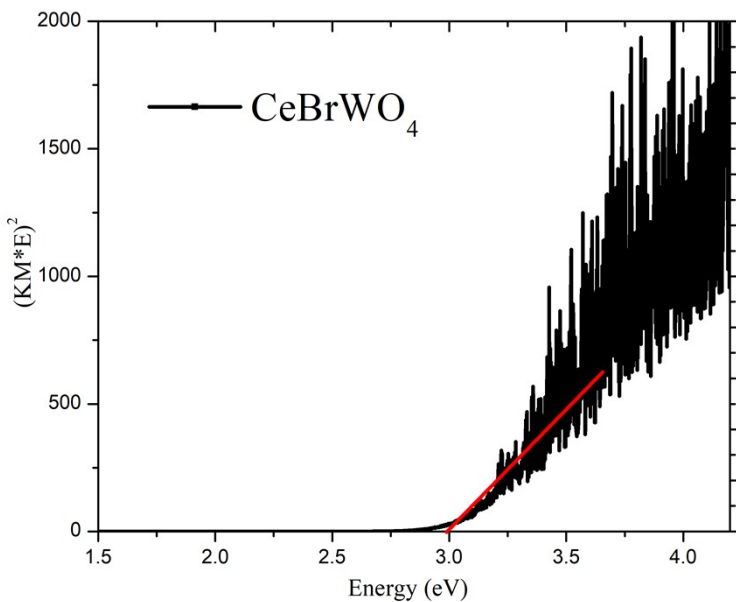


Figure S26. The allowed direct transitions of two CeBrWO₄ sample.

Reference:

- [1] I. Hartenbach, T. Schleid, S. Strobel and P. K. Dorhout, *Z. Anorg. Allg. Chem.*, 2010, **636**, 1183–1189.
- [2] T. Schleid and I. Hartenbach, *Z. Anorg. Allg. Chem.*, 2009, **635**, 1904–1909.
- [3] I. Hartenbach, S. Strobel, T. Schleid, K. W. Krämer and P. K. Dorhout, *Z. Anorg. Allg. Chem.*, 2009, **635**, 966–975.
- [4] L. H. Brixner, H. Y. Chen and C. M. Foris, *J. Solid State Chem.*, 1982, **45**, 80–87.
- [5] I. Hartenbach, H. Henning, T. Schleid, T. Schustereit and S. Strobel, *Z. Anorg. Allg. Chem.*, 2013, **639**, 347–353.
- [6] T. Schleid and I. Hartenbach, *Z. Kristallogr. Cryst. Mater.*, 2016, **231**, 449–466.
- [7] T. Schustereit, T. Schleid, H. A. Höppe, K. Kazmierczak and I. Hartenbach, *J. Solid State Chem.*, 2015, **226**, 299–306.
- [8] T. Schustereit, H. Henning, T. Schleid and I. Hartenbach, *Z. Naturforsch. B J. Chem. Sci.*, 2013, **68**, 616–624.
- [9] T. Schustereit, T. Schleid and I. Hartenbach, *Solid State Sci.*, 2015, **48**, 218–224.
- [10] C. Liu, Y. Xiao, H. Wang, W. Chai, X. Liu, D. Yan, H. Lin and Y. Liu, *Inorg. Chem.*, 2020, **59**, 1577–1581.
- [11] L.-T. Jiang, M.-Z. Li, X.-M. Jiang, B.-W. Liu and G.-C. Guo, *Dalton Trans.*, 2022, **51**, 6638–6645.
- [12] C. Liu, P. Hou, W. Chai, J. Tian, X. Zheng, Y. Shen, M. Zhi, C. Zhou and Y. Liu, *J. Alloys Compd.*, 2016, **679**, 420–425.
- [13] S. Al Bacha, S. Saitzek, E. E. McCabe and H. Kabbour, *Inorg. Chem.*, 2022, **61**, 18611–18621.
- [14] N. Zhang, S.-S. Han, Y. Xie, D.-L. Chen, W.-D. Yao, X. Huang, W. Liu and S.-P. Guo, *Inorg. Chem.*, 2023, **62**, 7681–7688.

- [15] J. Bao, W. Quan, Y. Ning, H. Wang, Q. Wei, L. Huang, W. Zhang, Y. Ma, X. Hu and H. Tian, *Inorg. Chem.*, 2023, **62**, 1086–1094.
- [16] Z. Zhijie, L. Deben, H. Hao, C. Yaoqing and X. Jiayue, *Inorg. Chem.*, 2023, **62**, 9240–9248.
- [17] Y. Chi, T.-F. Jiang, H.-G. Xue and S.-P. Guo, *Inorg. Chem.*, 2019, **58**, 3574–3577.
- [18] Y. Chi, L.-Z. Rong, N.-T. Suen, H.-G. Xue and S.-P. Guo, *Inorg. Chem.*, 2018, **57**, 5343–5351.
- [19] W. Zhou, W.-D. Yao, R.-L. Tang, H. Xue and S.-P. Guo, *J. Alloys Compd.*, 2021, **867**, 158879.
- [20] A. Sarkar, A. Das, S. Ash, K. V. Ramanujachary, S. E. Lofland, N. Das, K. Bhattacharyya and A. K. Ganguli, *Inorg. Chem.*, 2023, **62**, 9324–9334.
- [21] Y. Xiao, S.-H. Zhou, R. Yu, Y. Shen, Z. Ma, H. Lin and Y. Liu, *Inorg. Chem.*, 2021, **60**, 9263–9267.
- [22] X. Huang, S.-H. Yang, W. Liu and S.-P. Guo, *Inorg. Chem.*, 2022, **61**, 12954–12958.
- [23] V. Werner, U. Aschauer, G. J. Redhammer, J. Schoiber, G. A. Zickler and S. Pokrant, *Inorg. Chem.*, 2023, **62**, 6649–6660.
- [24] M. Zhou, K. Xiao, X. Jiang, H. Huang, Z. Lin, J. Yao and Y. Wu, *Inorg. Chem.*, 2016, **55**, 12783–12790.
- [25] M. Zhou, X. Jiang, X. Jiang, K. Xiao, Y. Guo, H. Huang, Z. Lin, J. Yao, C.-H. Tung, L.-Z. Wu and Y. Wu, *Inorg. Chem.*, 2017, **56**, 5173–5181.